

This discussion paper is/has been under review for the journal *Atmospheric Chemistry and Physics (ACP)*. Please refer to the corresponding final paper in *ACP* if available.

**Sulfur cycle and  
sulfate radiative  
forcing**

I.-C. Tsai et al.

# Sulfur cycle and sulfate radiative forcing simulated from a coupled global climate-chemistry model

I.-C. Tsai<sup>1</sup>, J.-P. Chen<sup>1</sup>, P.-Y. Lin<sup>1</sup>, W.-C. Wang<sup>2</sup>, and I. S. A. Isaksen<sup>3</sup>

<sup>1</sup>Department of Atmospheric Sciences, National Taiwan University, Taiwan

<sup>2</sup>Atmospheric Sciences Research Center, State University of New York at Albany, USA

<sup>3</sup>Department of Geosciences, University of Oslo, Norway

Received: 1 August 2009 – Accepted: 1 October 2009 – Published: 22 October 2009

Correspondence to: J.-P. Chen (jpchen@as.ntu.edu.tw)

Published by Copernicus Publications on behalf of the European Geosciences Union.

Title Page

Abstract

Introduction

Conclusions

References

Tables

Figures

◀

▶

◀

▶

Back

Close

Full Screen / Esc

Printer-friendly Version

Interactive Discussion

## Abstract

The sulfur cycle and radiative effects of sulfate aerosol on climate are studied with a Global tropospheric Climate-Chemistry Model in which chemistry, radiation and dynamics are fully coupled. Production and removal mechanisms of sulfate are analyzed for the conditions of natural and anthropogenic sulfur emissions. Results show that the 1985 anthropogenic emission doubled the global SO<sub>2</sub> and sulfate loadings from its natural value of 0.15 and 0.27 Tg S, respectively. Under natural conditions, the fraction of sulfate produced in-cloud is 87%, and the lifetime of SO<sub>2</sub> and sulfate are 1.8 and 4.0 days, respectively; whereas with anthropogenic emissions, changes in in-cloud sulfate production are small, while SO<sub>2</sub> and sulfate lifetimes are significant reduced (1.0 and 2.4 days, respectively). The doubling of sulfate results in a direct radiative forcing of  $-0.32$  and  $-0.14$  W m<sup>-2</sup> under clear-sky and all-sky conditions, respectively, and a significant first indirect forcing of  $-1.69$  W m<sup>-2</sup>. The first indirect forcing is sensitive to the relationship between aerosol concentration and cloud droplet number concentration. Two aspects of chemistry-climate interaction are addressed. Firstly, the coupling effects lead to 10% and 2% decreases in sulfate loading, respectively, for the cases of natural and anthropogenic added sulfur emissions. Secondly, only the indirect effect of sulfate aerosols yields significantly stronger signals in changes of near surface temperature and sulfate loading than changes due to intrinsic climate variability, while other responses to the indirect effect and all responses to the direct effect are weak.

## 1 Introduction

Aerosol particles affect the Earth's energy budget directly by absorbing or scattering short-wave and long-wave radiation, and indirectly by influencing the structure and radiative properties of clouds through acting as cloud condensation nuclei and ice nuclei (Twomey, 1974; Albrecht, 1989). The perturbation of aerosols is believed to have significant impacts on climate, especially on regional scales (Ghan et al., 2001; Jones et

## Sulfur cycle and sulfate radiative forcing

I.-C. Tsai et al.

Title Page

Abstract

Introduction

Conclusions

References

Tables

Figures

◀

▶

◀

▶

Back

Close

Full Screen / Esc

Printer-friendly Version

Interactive Discussion



al., 2001; Williams et al., 2001; Rotstajn and Penner, 2001; Ramanathan, 2001; Andersen, 2003; IPCC, 2007). Although numerous studies have estimated aerosol direct and indirect effects, the results are highly uncertain (IPCC, 2007; Lohmann, 2005). IPCC (2007) for instance, reported that the global annual mean radiative forcing of aerosol direct effect is about  $-0.4 \text{ W m}^{-2}$  while for the first indirect effect (or the cloud albedo effect) the forcing ranges from  $-0.3$  to  $-1.8 \text{ W m}^{-2}$ .

Sulfate particle is an important component of atmospheric aerosols. Many studies have discussed the importance of the sulfur cycle (Rodhe and Isaksen, 1980; Chin et al., 1996, 2000; Feichter et al., 1996; Koch et al., 2001; Iversen and Seland, 2002; Liao et al., 2003, Berglen et al., 2004). The key species in tropospheric sulfur cycle are the gaseous DMS (dimethylsulfide) and  $\text{SO}_2$ , and sulfate via their oxidation by various oxidants including  $\text{O}_3$ , OH,  $\text{H}_2\text{O}_2$ ,  $\text{HO}_2\text{NO}_2$  and  $\text{NO}_3$ .

Many chemical transport models (CTMs) have been developed to simulate the sulfur cycles using prescribed (offline) meteorology to drive the chemistry. Another approach has been to use prescribed aerosol for calculating radiative forcing in global climate models (e.g. Mitchell et al., 1995; Chou, 2004; Chen and Penner, 2005; Gu et al., 2006; Jones et al., 2007). Since interactions with the meteorological fields (e.g. cloud removal) are crucial to the sulfur cycle evolution, and although such simulations do include the impact of aerosol radiative forcing on atmospheric circulation, the lack of consistency in considering non-linear in situ production of sulfate aerosols (Berglen et al., 2004) introduces large uncertainties in sulfur cycle estimates. Many studies indicated that feedbacks might be more influential than expected (Kaufman and Freaser, 1997; Cerveny and Bailing, 1998; Audiffren et al., 2004; Resenfeld, 2000), therefore, models that do not include coupled chemistry, radiation and dynamics may have large errors in the estimates of the feedback mechanisms occurring in the climate system and impact the model results (Zhang, 2008).

Recently, efforts have been devoted to the modeling of coupled climate-chemistry system in order to gain a better understanding of aerosol-cloud-climate interactions (Eyring et al., 2005; Patrick Jöckel et al., 2005). The impacts of coupling are still

## Sulfur cycle and sulfate radiative forcing

I.-C. Tsai et al.

Title Page

Abstract

Introduction

Conclusions

References

Tables

Figures

◀

▶

◀

▶

Back

Close

Full Screen / Esc

Printer-friendly Version

Interactive Discussion



**Sulfur cycle and sulfate radiative forcing**

I.-C. Tsai et al.

[Title Page](#)[Abstract](#)[Introduction](#)[Conclusions](#)[References](#)[Tables](#)[Figures](#)[⏪](#)[⏩](#)[◀](#)[▶](#)[Back](#)[Close](#)[Full Screen / Esc](#)[Printer-friendly Version](#)[Interactive Discussion](#)

very uncertain, limited by the complexity of mechanisms considered in the model. For example, Mickley et al. (1999), considering only O<sub>3</sub> impacts on radiation, estimated that the difference of O<sub>3</sub> radiative forcing between offline and online calculations is about 2%. However, Shindell et al. (2001) also used online model to illustrate that the OH concentration could be reduced by about 10%, which would be significant to many chemical processes.

In this study we incorporated an interactive tropospheric sulfur chemistry scheme into a global climate-chemistry model (GCCM) (Wong et al., 2004) to estimate radiative forcing of sulfate aerosols, including direct aerosol effect and aerosol-cloud albedo effect. Furthermore, by comparing simulations with and without the coupling of aerosol radiative forcing, we examined the meteorological responses to the forcing as well as feedbacks to the meteorology and subsequently to the aerosol fields.

## 2 Description of the model and the simulations

### 2.1 Global climate-chemistry model

The GCCM was developed by incorporating the University of Oslo tropospheric photochemical scheme (Isaksen and Hov, 1987; Berntsen and Isaksen, 1997) into the National Center for Atmospheric Research Community Climate Model (CCM3) with modification by the group of State University of New York at Albany (Wang et al., 1995; Wong and Wang, 2000, 2003). This model has been used for simulating tropospheric chemistry and the effect of ozone on radiation. In spite of cold biases of about 4–12 K in the polar regions, and small dry biases during July to August in Northern Hemispheric mid-latitudes, this model can reproduce reasonable inter-annual variability of the tropospheric system (Hack et al., 1998; Wong and Wang, 2003).

However, in Wong et al. (2004) the sulfur chemistry that is important for the study of aerosol effects was not included because their focus was on ozone and its impact.

We have now incorporated the sulfur and oxidant chemistry scheme of Berglen et al.

**Sulfur cycle and sulfate radiative forcing**

I.-C. Tsai et al.

(2004) into GCCM, to take into account the interaction with the sulfate chemistry. Performing on-line calculations provide consistent estimates of chemical distribution and changes of gaseous- and aqueous-phase compounds. Four new species, DMS, SO<sub>2</sub>, MSA and SO<sub>4</sub><sup>2-</sup> (sulfate), are added. The new processes considered are: emission of SO<sub>2</sub>, DMS and SO<sub>4</sub><sup>2-</sup>, dry and wet deposition of SO<sub>2</sub>, MSA and SO<sub>4</sub><sup>2-</sup>, and gaseous- and aqueous-phase chemical reactions, as shown in the schematics of Fig. 1. The key gas and aqueous phase reactions for the sulfur cycle are listed in Table 1, and more details can be found in Berglen et al. (2004). Note that in the GCCM sea-surface temperatures are specified according to the results from the Atmospheric Model Inter-comparison Project 2 (AMIP 2) (Gates et al., 1999).

**2.2 Emissions**

The global emissions of pollutants except sulfur species are based on IPCC 2001 (Ox-Comp Y2001), with annual mean values rescaled to 1990 emission following Wong et al. (2004). Sulfur emissions include anthropogenic emission sources following the GEIA 1985 inventory (Benkovitz et al., 1996), ship emission from Endresen et al. (2003), biomass burning from Spiro et al. (1992) and Graft et al. (1997). Table 2 shows the total emission strengths from each source. It is assumed that 5% of anthropogenic sulfur is emitted as sulfates while the rest as SO<sub>2</sub> (Langner and Rodhe, 1991).

Natural sulfur sources include volcanic emission (Spiro et al., 1992) and DMS emission from the ocean (Kettle et al., 1999; Kettle and Andreae, 2000). The DMS flux is calculated with specified seawater DMS concentrations using transport parameterization of Liss and Merlivat (1986):

$$F = V_k \times (C_{\text{DMS,air}}/H - C_{\text{DMS,ocean}}) \quad (1)$$

where  $V_k$  is parameterized transport velocity,  $C_{\text{DMS,air}}$  is DMS concentration in air,  $H$  is Henry constant for DMS, and  $C_{\text{DMS,ocean}}$  is DMS concentration in seawater. The amount of SO<sub>2</sub> produced from DMS conversion stays in a narrow range of 21.0 to 21.8 Tg S (terra grams of sulfur) per year among all simulations that are conducted

[Title Page](#)[Abstract](#)[Introduction](#)[Conclusions](#)[References](#)[Tables](#)[Figures](#)[◀](#)[▶](#)[◀](#)[▶](#)[Back](#)[Close](#)[Full Screen / Esc](#)[Printer-friendly Version](#)[Interactive Discussion](#)

in this study (based on the assumptions made for the products in Reaction (R3) in Table 1).

## 2.3 Cloud effective radius

As mentioned in previous sections, the sulfate particles could serve as cloud condensation nuclei and modify cloud drop number concentration hence cloud radiative properties, leading to the cloud albedo effect. However, similar to that done in many other GCMs, the previous version of GCCM applies prescribed cloud droplet effective radii of  $5\ \mu\text{m}$  over continents and  $10\ \mu\text{m}$  over oceans for the radiation calculation. Such an approach only grossly represents the spatial distribution of aerosol influences and certainly cannot reflect response to the change of aerosols. Based on observations, Boucher and Lohmann (1995) provided improvement with empirical formulas that link the effective radii of cloud drops to sulfate mass loading:

$$N_C = \exp(a_0 + a_1 * \log(M_{\text{SO}_4})) \quad (2)$$

where  $M_{\text{SO}_4}$  is the sulfate mass loading in  $\mu\text{g}/\text{m}^{-3}$  and  $N_C$  is the cloud droplet number concentration in  $\text{cm}^{-3}$ , and different values of coefficients  $a_0$  and  $a_1$  are provided for the continental and oceanic conditions. However, their formulas tend to overestimate the number concentration of cloud drops, thus underestimate the effective radii, especially over the oceans. That will lead to overestimated sulfate radiative forcing. Quaas and Boucher (2005) made an adjustment to correct for this underestimate and provided the coefficients  $a_0=3.9$  and  $a_1=0.2$ , and these are the values adopted for this study. The coefficients given by Boucher and Lohmann (1995) will also be tested and presented in the discussion section. The effective radius  $r_e$  can be calculated as:

$$r_e = \left( \frac{3w_l}{4\pi\rho_w k N_C} \right)^{1/3} \quad (3)$$

where  $w_l$  is cloud water content,  $\rho_w$  is the density of water, and  $k$  is a modification coefficient to account for the difference between the mean volume radius ( $r_v$ ) and  $r_e$  of

## Sulfur cycle and sulfate radiative forcing

I.-C. Tsai et al.

Title Page

Abstract

Introduction

Conclusions

References

Tables

Figures

◀

▶

◀

▶

Back

Close

Full Screen / Esc

Printer-friendly Version

Interactive Discussion



cloud droplets, which is assumed as 0.67 over continents and 0.8 over oceans according to Martin et al. (1994).

## 2.4 Simulations

Two sets of simulations are conducted to estimate the sulfate aerosols direct and indirect effects. Simulations N0, N1 and N2 apply only natural sulfur emissions (i.e. DMS and volcanic SO<sub>2</sub> emissions), whereas simulations A0, A1 and A2 take additional anthropogenic sulfur emissions. The degree of coupling the aerosol effects is indicated by the numbers after “N” and “A”, where “0” denotes no sulfate radiative effects, “1” denotes only sulfate direct effect, and “2” indicates both sulfate direct effect and the first indirect effect. Six months spin-off were conducted for N0, and then used to run other cases for a period of 13 years. For analysis, we used results from the last 5 years. Monthly meteorological fields and trace gas concentrations were examined to ensure that near-steady-state climate conditions are reached.

All simulations apply a horizontal resolution of T42 (equivalent to 2.8° × 2.8°) and 18 vertical layers from the surface to about 2.5 hPa. The time step used is 20 min, with the exception that shortwave and long-wave radiation processes are calculated hourly.

## 3 Analyses

In the following we first briefly compare the global distribution of simulated meteorological fields and sulfur species with observational data to check the general model performance using results from the A2 and N2 simulations. Next, sulfate aerosol forcing as well as the effect of coupling will be discussed for the simulations.

### 3.1 Global distributions

As a first step of verifying GCCM performance, we compared the meteorological fields from the A2 simulation to those of the climatological data. Near-surface mean temper-

## Sulfur cycle and sulfate radiative forcing

I.-C. Tsai et al.

Title Page

Abstract

Introduction

Conclusions

References

Tables

Figures

◀

▶

◀

▶

Back

Close

Full Screen / Esc

Printer-friendly Version

Interactive Discussion



ature and wind fields are compared with the 1979–2005 climatology of the NCEP-DOE Reanalysis 2 (NCEP RE2), whereas surface precipitation is compared with that of the Global Precipitation Climatology Project (GPCP, 1979–present). Figure 2a–d show the convergence over tropical regions, divergence over 30° N and 30° S and the distribution of isothermal of A2 results are similar to NCEP RE2 climatology. The pattern of surface precipitation simulated with GCCM is generally quite similar to those of GPCP, except that the model result is wetter over the tropics and drier over mid-latitude Pacific Ocean (Fig. 2e and f). Since the model sea surface temperature is prescribed, air temperature above the ocean is close to the climatology.

Figure 3a shows the simulated global distribution of SO<sub>2</sub> column concentration from simulation A2. Note that areas of high concentrations near or downwind of major anthropogenic emission hot spots occur in central Europe, eastern United States, eastern China, and Russia. There are also secondary maxima in southern Africa, South America and Indonesia due to biomass burning and volcanic eruptions. These patterns are in general agreement with GOME satellite observation reported in Khokhor et al. (2004). Differences exist in a few places, partly because the 1985 distribution is for a different time period than the GOME observations, for which data are available only after 1995. Besides the differences in anthropogenic emission inventory, the discrepancies may also result from the use of climatological volcanic emissions in our simulations, which might not reflect major volcanic eruptions during 1996–2002 (Khokhor et al., 2004). Nevertheless, the GCCM simulation captured the general features of SO<sub>2</sub> spatial distribution.

The sulfate distribution has a rather similar pattern as SO<sub>2</sub> (Fig. 3b), except that it spreads over a wider area, likely due to time lag of chemical conversion from SO<sub>2</sub> which allows more time for atmospheric dispersion, since it is a secondary compound, while SO<sub>2</sub> is a primary compound with shorter lifetime (Berglen et al., 2004). Unfortunately, the simulated global distribution of sulfate is difficult to verify, as relevant observation is scarce. Satellite observations of aerosol optical depth seem to be pertinent, but they contain contribution from non-sulfate particles such as mineral dust and soot particles,

## Sulfur cycle and sulfate radiative forcing

I.-C. Tsai et al.

Title Page

Abstract

Introduction

Conclusions

References

Tables

Figures

⏪

⏩

◀

▶

Back

Close

Full Screen / Esc

Printer-friendly Version

Interactive Discussion





**Sulfur cycle and sulfate radiative forcing**

I.-C. Tsai et al.

[Title Page](#)[Abstract](#)[Introduction](#)[Conclusions](#)[References](#)[Tables](#)[Figures](#)[◀](#)[▶](#)[◀](#)[▶](#)[Back](#)[Close](#)[Full Screen / Esc](#)[Printer-friendly Version](#)[Interactive Discussion](#)

so their global features can be distinctly different from the sulfate distribution. Another way to check the correctness of our sulfur-cycle calculations is to compare with results from other models that also applied the 1985 emission inventory. Global model studies referred to in Berglen et al. (2004) and in the AeroCom project (Schulz et al., 2006) revealed large differences in current estimates of sulfate burden. The mean global loading of SO<sub>2</sub> and sulfate from our A2 simulation are 0.29 and 0.54 Tg S, respectively, as listed in Table 3. These global loadings are on the low side but within the range of other model results.

In the following discussion we analyze the contribution of sulfur species from different emission sources and the production mechanisms of sulfate. The natural SO<sub>2</sub> concentrated over the northern high latitudes and tropical regions to the east of Indonesia (Fig. 3c) are mainly from volcanic emissions. Annual global production of SO<sub>2</sub> from DMS is about 21.8 Tg S, much higher than the 8 Tg S per year from volcanic emissions (Table 2). However, DMS is released in the lower troposphere, so the SO<sub>2</sub> formed from DMS may experience stronger surface removal by dry deposition or conversion to sulfate by aqueous-phase reactions where liquid clouds are prevalent. Volcanic emission is actually a more dominant source of global SO<sub>2</sub>, typically injected into the upper troposphere (Fig. 4c). Thus, the global distribution of column SO<sub>2</sub> in Fig. 3c does not show obvious signature of DMS production zones but rather concentrate over the volcanic active areas. But from the vertical distribution shown in Fig. 4c one may notice the presence of DMS-converted SO<sub>2</sub> that stays near the surface over mid-latitude oceans (mainly around 40° S and some over 10–60° N).

Natural sulfate also spreads over a much wider area than SO<sub>2</sub> distribution (Fig. 3d). This feature can also be seen in the vertical distributions in Fig. 4d. Figure 3e gives the ratio of natural to total SO<sub>2</sub> (N2 to A2), and from it one can see that anthropogenic sources dominate SO<sub>2</sub> over all the populated continents and adjacent oceans. Natural sources account for less than 50% of the SO<sub>2</sub> on most portion of the populated continents, and the ratio may decrease to less than 10% over major urban and industrial regions. The ratios for sulfate (Fig. 3f) are generally similar, with natural contributions

dominating only over the polar regions and some remote oceans. The contrast of natural versus anthropogenic contributions of  $\text{SO}_2$  is even sharper at the surface layer. Figure 3g show that more than 90% of the surface  $\text{SO}_2$  over most of the land areas is of anthropogenic origin. Over the remote oceans one can see the dominance of anthropogenic emissions on  $\text{SO}_2$  concentration over major shipping routes. But the surface distribution of sulfate (Fig. 3h) does not retain the features of shipping corridors, again indicating the time lag in  $\text{SO}_2$  to sulfate conversion and more efficient sulfate dispersion.

The vertical distribution of sulfur depends on the location of emission sources as well as atmospheric transport and removal processes. As shown in Fig. 4e and f, the fraction of anthropogenic  $\text{SO}_2$  over mid-latitude Northern Hemisphere exceeds 90% near the surface, and the value remains above 50% up to the 500-hPa level. In the Southern Hemisphere, the highest anthropogenic fraction is at the surface around  $20^\circ\text{S}$ , while the 50% isopleth stays below the 900-hPa level. Fraction of sulfate from anthropogenic contributions generally exceeds that of  $\text{SO}_2$ . As shown in Fig. 4f, the 50% isopleths enclose a large portion of the troposphere and may reach an altitude of 200 and 400 hPa over the Northern and Southern Hemisphere, respectively. Globally, natural emissions are responsible for slightly more than one half of the total for both sulfur species (see Table 3).

The net sulfate loading is determined by the rates of production (direct emission and oxidation from  $\text{SO}_2$  in air and clouds) and removal (dry and wet deposition). A brief overview of the magnitude of each process may facilitate the discussion of the coupling effect in later sections. According to the N2 simulation, annual production of  $\text{SO}_2$  is 29.8 Tg S (including volcanic emission and conversion from DMS), whereas under polluted condition (A2) the total production is 102.4 Tg S. Conversion of  $\text{SO}_2$  into sulfate occurs mainly in clouds. For natural conditions, 51% are from ozone oxidation and 34% are from  $\text{H}_2\text{O}_2$  oxidation, whereas gas-phase oxidation by OH radical accounts for about 13%, and the rest is by other in-cloud reactions. With the addition of anthropogenic emissions (A2), the proportions become 56% by ozone, 30% by  $\text{H}_2\text{O}_2$  and

**Sulfur cycle and sulfate radiative forcing**

I.-C. Tsai et al.

Title Page

Abstract

Introduction

Conclusions

References

Tables

Figures

◀

▶

◀

▶

Back

Close

Full Screen / Esc

Printer-friendly Version

Interactive Discussion



11% by OH. Such a change of proportions indicates that the increase of tropospheric ozone due to human pollution significantly enhances in-cloud production of sulfate. The concentration of  $\text{H}_2\text{O}_2$  and OH also increased somewhat, leading to enhancement of sulfate production both by 2.8 folds. But such an enhancement is actually less than the 3.4 times increase of  $\text{SO}_2$  productions (A2 versus N2), and this implies that  $\text{H}_2\text{O}_2$  and OH are probably the predominant limiting agent in the oxidation reactions. On the other hand, the enhancement of sulfate production by ozone oxidation (3.6 times) is close to that of  $\text{SO}_2$  production, indicating that ozone is usually not the limiting agent. The fraction of in-cloud sulfate production from our A2 results (89%) is significantly higher than in several global CTMs. For example, the values estimated by Chin et al. (2000), Restad et al. (1998), Koch et al. (1999) and Roelofs et al. (1998) range from 64 to 78%. However, our value is closer to the 84 to 85% by Berglen et al. (2004) and Chin et al. (1996). It is also similar to the 86% in Lelieveld (1993) who performed the estimation based on global cloud climatology and specified chemical reaction rates. As GCCM applied essentially the same chemical scheme as Berglen et al. (2004), the discrepancy between them is likely due to differences in meteorology, such as the amount of liquid cloud and transport processes. Under natural conditions, the removal of sulfate from the atmosphere is mainly via wet deposition, and only 7.7% is by dry deposition. For polluted conditions, the proportion by dry deposition increases to 9.4%, since most of the anthropogenic  $\text{SO}_2$  are emitted close to the surface, so they are more susceptible to dry deposition than natural emissions from volcanic eruptions and secondary  $\text{SO}_2$  from DMS.

Dividing the global loading given in Table 3 by the overall rate of destruction (same as rate of production under steady state), we are able to estimate the lifetime of  $\text{SO}_2$ , which is 1.8 days under natural conditions (N2), and 1.0 days under polluted conditions (A2). For comparison, we listed  $\text{SO}_2$  lifetime under polluted conditions from other studies listed in Table 3, which are 1.1, 1.3, 2.0, 2.6 and 2.4 days in Berglen et al. (2004), Chin et al. (1996), Restad et al. (1998), Koch et al. (1999) and Roelofs et al. (1998), respectively. The lifetime of sulfate is estimated to be 4.0 and 2.4 days for the unpol-

**Sulfur cycle and sulfate radiative forcing**

I.-C. Tsai et al.

Title Page

Abstract

Introduction

Conclusions

References

Tables

Figures

◀

▶

◀

▶

Back

Close

Full Screen / Esc

Printer-friendly Version

Interactive Discussion



luted (N2) and polluted (A2) conditions. Sulfate lifetime from A2 is significantly lower than from the aforementioned CTM calculations, which range from 3.7 to 5.7 days. The overall lifetime of sulfur (SO<sub>2</sub> plus sulfate) is 5.3 days in N2 and 2.9 days in A2.

The atmospheric lifetime is determined by its largest sink, so for SO<sub>2</sub> the dominating factor is in-cloud oxidation, while for sulfate wet deposition is the most important. The large variation of sulfur lifetime among models shown above indicates high uncertainties in the simulation of sulfur cycle, and the uncertainties are mainly a result of differences in formulating cloud-related sink processes. As mentioned previously, the in-cloud oxidation of SO<sub>2</sub> in GCCM is stronger than in other models, so it is not surprising that our calculation of SO<sub>2</sub> lifetime is shorter. Furthermore, this also implies that the amount of cloudwater (for the oxidation to take place) could be quite different among models. Apparently, different climate models, even with prognostic clouds, cannot get consistent cloud water and precipitation (cf. Lau et al., 1996). A stronger in-cloud production also means a shorter lifetime for sulfate (larger production rate), which partly explain why the value from our model is significantly lower. The shorter lifetime of sulfate could also mean a stronger precipitation which lead to stronger wet deposition. Again, precipitation among climate models are very different, and the value (3.2 mm day<sup>-1</sup>) obtained in GCCM is on the high side compared to various GCM results from AMIP (Lau et al., 1996). We find that the coupling of sulfate radiative forcing, which will be discussed later, caused a reduction of mass loading hence shortened the lifetime of sulfate, and the reduction is about 10% for the natural conditions (N2 versus N0) and 2% for the polluted conditions (A2 versus A0). From budget analysis we found that the reduction of sulfate loading in A2 versus A0 is due to a stronger wet deposition, which is related to the stronger precipitation (see Table 5), as well as a weaker aqueous-phase production, which is a consequence of lower SO<sub>2</sub> concentration (see Table 3). The lower SO<sub>2</sub> concentration is associated with a stronger dry deposition, which in turn is related to a weaker vertical transport in the fully-coupled model such that more SO<sub>2</sub> stays near the surface thus susceptible to deposition. The changes occurred between the N2 versus N0 simulations are very similar. The calculated distri-

## Sulfur cycle and sulfate radiative forcing

I.-C. Tsai et al.

Title Page

Abstract

Introduction

Conclusions

References

Tables

Figures

◀

▶

◀

▶

Back

Close

Full Screen / Esc

Printer-friendly Version

Interactive Discussion



butions and variation of oxidants (e.g. O<sub>3</sub>, OH), which are responsible for atmospheric conversion of SO<sub>2</sub> to sulfate are similar to what was presented by Wong et al. (2004).

### 3.2 Sulfate radiative forcing

In this section we present the direct effect and the first indirect effect of sulfate aerosol forcing. To determine radiative forcing from anthropogenic sulfate aerosols, we simply take the difference between the A-series and N-series calculations. The distribution of radiative forcing at the surface is very similar to the distribution at the top of the atmosphere (TOA), only the latter is therefore discussed.

Direct forcing for both clear-sky and all-sky conditions can be obtained from either the A1–N1 or the A2–N2 results. Note that sulfate in A0 and N0 does not affect radiation, so the differences of radiative forcing between these two simulations arise from the influences of ozone chemistry and from model internal variability, which will be further elaborated later. Globally, as shown in Table 4, aerosol direct forcing is about  $-0.32 \text{ W m}^{-2}$  at TOA, which is more significant than the  $-0.05 \text{ W m}^{-2}$  by ozone from the A0–N0 results. Figure 5 compares the mass loading and direct forcing of sulfate from various models, and the values from GCCM are well within the range of others. Direct forcing under all-sky conditions may be represented by the A1–N1 forcing, as neither A1 nor N1 considered the sulfate indirect effect. From Table 4 we can see that the global direct forcing reduces to  $-0.14 \text{ W m}^{-2}$  for all-sky conditions.

For the indirect forcing of anthropogenic sulfate, it may be represented by the differences between the A2 and N2 results. Note that, because the cloud effective radii are prescribed in A0, A1, N0 and N1 simulations, it is not appropriate to use A2–A0 or N2–N0 to represent the indirect effect of sulfate. Figure 6a shows the distribution of total sulfate forcing based on A2–N2 results. As the indirect forcing is much higher than the direct forcing (see Table 4), one may regard them as all from the indirect effect. The indirect forcing not only is much stronger than the direct forcing but also extends to areas that are quite far away from the pollution centers, such as a large portion of the Atlantic and significant portion of other oceans. The highest regional indirect forc-

## Sulfur cycle and sulfate radiative forcing

I.-C. Tsai et al.

Title Page

Abstract

Introduction

Conclusions

References

Tables

Figures

◀

▶

◀

▶

Back

Close

Full Screen / Esc

Printer-friendly Version

Interactive Discussion



**Sulfur cycle and sulfate radiative forcing**

I.-C. Tsai et al.

ing may reach  $-20 \text{ W m}^{-2}$  over eastern North America and southeastern China. But there are also areas experiencing positive forcing, mostly over the continents around the regions of strong negative forcing, possibly resulting from regional adjustment in the dynamics and cloud fields. These positive forcing leads to a smaller global indirect forcing that averages to about  $-1.69 \text{ W m}^{-2}$ . Similar to the approach applied earlier, alternative estimation can be derived by deducting the N2–N0 forcing from that of A2–A0 for all-sky conditions, which gives a global indirect forcing of  $-1.56 \text{ W m}^{-2}$ . This value is rather close to that from the A2–N2 results, indicating the robustness of its value.

To provide a broader perspective, we compare our model results with other studies, noting that there are many differences among the models. IPCC (2007) summarized results from different estimations and suggested the range of  $-0.1$  to  $-0.9 \text{ W m}^{-2}$  for the direct effect, and  $-0.3$  to  $-1.8 \text{ W m}^{-2}$  for the first indirect effect. Our estimation of the direct effect is within the range and the indirect effect is on the high end. However, our simulations consider only sulfate aerosols, while some of those reported in IPCC (2007) may contain other aerosol types.

### 3.3 Climate responses to sulfate forcing

Aerosol forcing affects the energy budget thus the dynamics of the atmosphere, which in turn influence clouds and precipitation then consequently the feedback to the radiation field. Figure 6b shows the changes in near-surface air temperature due to direct and indirect forcing according to the results of A2–N2. Significant cooling can be found over (but not confined to) the three main areas of pollution sources: eastern China, Eastern Europe, and eastern United States. One can also find significant warming over areas such as northern North America, mid-north Africa, and northern Australia. The temperature change pattern does not have a one-to-one correspondence with the pattern of radiative forcing that is shown in Fig. 6a, indicating that the radiation field has interactions with the dynamic and cloud fields.

The global mean responses of several key climate parameters are summarized in

[Title Page](#)[Abstract](#)[Introduction](#)[Conclusions](#)[References](#)[Tables](#)[Figures](#)[⏪](#)[⏩](#)[◀](#)[▶](#)[Back](#)[Close](#)[Full Screen / Esc](#)[Printer-friendly Version](#)[Interactive Discussion](#)

**Sulfur cycle and sulfate radiative forcing**

I.-C. Tsai et al.

[Title Page](#)[Abstract](#)[Introduction](#)[Conclusions](#)[References](#)[Tables](#)[Figures](#)[◀](#)[▶](#)[◀](#)[▶](#)[Back](#)[Close](#)[Full Screen / Esc](#)[Printer-friendly Version](#)[Interactive Discussion](#)

Table 5. The direct forcing (A1–N1) leads to a decrease of global near-surface air temperature by about 0.02 K, but this change is even smaller than the  $-0.04$  K forcing from ozone changes estimated from the A0–N0 results. This indicates that the direct forcing is probably too weak compared to other forcing mechanisms. On the other hand, the 0.09 K cooling due to both the direct and indirect effects (A2–N2) is larger than that from A1–N1, and apparently most of it is from the indirect effect. Note that the change in surface air temperature here is underestimated because of the fixed ocean surface temperature. The indirect effect of anthropogenic sulfate also leads to an increase of cloud coverage by 0.04% and a depression of precipitation by 0.21% due to dynamic feedbacks. The contrasting change in cloud coverage and precipitation implies that the additional clouds are mostly non-precipitating type. But these small changes are probably not particularly meaningful when considering the internal variability of the model as will be discussed later. The responses of global mean cloud amount due to the direct forcing of sulfate (A1–N1) are more significant even though the forcing is weaker as compared with the indirect forcing.

The GCM responses to sulfate forcing are more significant on the regional scale and may even lead to changes in the monsoon system. In East Asia for example, weaker summer monsoon and stronger winter monsoon emerge under the forcing of anthropogenic sulfate, leading to reduced moisture flux from the ocean to the East Asian continent in both seasons. The changes are in many aspects similar to those simulated with the regional coupled climate-chemistry model by Huang et al. (2007) who found a regional radiative forcing of  $-4.08 \text{ W m}^{-2}$ , leading to a cooling of the mean surface temperature by 0.35 K and reduced cloud fraction by 0.8% and precipitation by more than 10%; whereas the values we obtained are  $-3.99 \text{ W m}^{-2}$ ,  $-0.24$  K,  $-1\%$ , and  $-5.3\%$ , respectively. In addition, the two simulation results share similar geographic distribution of reduced precipitation, with the largest change occurring over South-East Asia during summer and winter. The main calculated features of monsoon flow and precipitation changes over East Asia are reasonably consistent with the sulfate forcing effects reported by Liu et al. (2009) who performed global simulations using CAM 3.0



with assimilated aerosols. In other regions the responses to sulfate forcing may be quite different, and the details are quite convoluted and tedious thus will not be elaborated here.

### 3.4 Effect of coupling on sulfate chemistry

5 The climate responses discussed above will also alter the transformation, transport, and removal of aerosols, thus forming feedback loops. Because atmospheric sulfate is formed mainly in liquid clouds (about 89% in A2), while its removal is mainly by precipitation scavenging (about 75% in A2), any change in the cloud fields could affect sulfate loading. In addition, the changes in circulation and other parameters such as humidity and actinic flux due to sulfate forcing may influence the transport, dry deposition as well as chemical formation of sulfate. These feedbacks exist only when the sulfur chemistry is coupled to processes in the climate model.

10 However, to examine the sensitivity of the sulfur cycle to sulfate forcing, it is not proper to compare simulation set of A2–N2 (or A1–N1, A0–N0) as done earlier, because it would only reflect the large differences in emissions. A better comparison can be performed between either the A-series or N-series of simulations, as their emissions are the same but the degrees of coupling of sulfate forcing are different. Note that A0 and A1 simulations do include cloud forcing but the calculations are based on specified effective radii. From Table 3 we can see that SO<sub>2</sub> loading remains quite steady among the N-series of simulations, and varies only slightly among the A-series of simulations. Sulfate loading under natural conditions varies more significantly, with the N2 sulfate loading being 10% less than that from N0. Under polluted conditions, sulfate calculated with the fully-coupled A2 simulation (0.54 Tg S) is only about 2% less than that (0.55 Tg S) from the less coupled simulations (i.e. A1 and A0). The main cause of these differences in sulfate loading is the change in dry deposition, which should be related to the change in circulation and atmospheric stability that regulates the vertical transport. Take the 10% reduction from N0 to N2 for example, over 6% is due to enhanced dry deposition, while the rest is due to increased wet deposition (mainly because of more

## Sulfur cycle and sulfate radiative forcing

I.-C. Tsai et al.

Title Page

Abstract

Introduction

Conclusions

References

Tables

Figures

◀

▶

◀

▶

Back

Close

Full Screen / Esc

Printer-friendly Version

Interactive Discussion





precipitation in N0) as well as decreased conversion from SO<sub>2</sub> oxidation. However, these reductions may be too small to cause significant feedbacks to radiative forcing.

## 4 Discussions

Earlier we showed that sulfate aerosols may exert forcing on several climate parameters including surface temperature, winds, clouds and precipitation. The indirect forcing due to cloud albedo effect seems to be quite significant from the fully coupled A2–N2 results. However, as indicated from the A1–N1 results, the direct forcing of anthropogenic sulfate is so weak that its signal might not be distinguishable from other effects that have similar or greater magnitudes. For example, the change of gas-phase chemistry (i.e. increasing ozone) due to anthropogenic pollutants could induce similar temperature change as indicated by the A0–N0 results where aerosol forcing is not considered. It is important to establish whether the climate responses we saw in the previous section are truly from the aerosol effects or simply noises. Nevertheless, the A2–N2 results do show a strong signal of responses to the indirect forcing by sulfate, even though the results do contain uncertainties as discussed in the following.

To eliminate the possibility that differences between simulations shown in Tables 4 and 5 simply are due to internal climate variability of the model, we need to understand how large such an internal variability is. In Fig. 7 the response of several parameters is plotted against their internal variability. The response is defined as the difference between two sets of simulations, whereas the internal variability is defined as the seasonal or annual anomaly during the 5 years of simulation time using the second set of simulation as the reference. For example, with the mean temperature difference of A2–N2 as the response, the deviation of annual mean temperature of the subtrahend, N2, from their 5-year average will represent the internal variability. Note that in the above example one may also choose the A2 results to represent the internal variability, and the differences between this and the above approaches will be discussed. The month-to-month plots are similar, thus we show only the annual values. Figure 7a shows

### Sulfur cycle and sulfate radiative forcing

I.-C. Tsai et al.

Title Page

Abstract

Introduction

Conclusions

References

Tables

Figures

◀

▶

◀

▶

Back

Close

Full Screen / Esc

Printer-friendly Version

Interactive Discussion



**Sulfur cycle and sulfate radiative forcing**

I.-C. Tsai et al.

that the responses of TOA radiation to sulfate indirect forcing (A2–N2) lies consistently between  $-1.5$  and  $-2.0 \text{ W m}^{-2}$ , and they are significantly larger than the internal variability which lies within  $\pm 0.2 \text{ W m}^{-2}$ . But for the ozone forcing (A0–N0) or the sulfate direct forcing (A1–N1) the responses are of similar magnitude as the internal variability.

Furthermore, the spread across the one-to-one line indicates they are not consistently larger or smaller than the internal variations. These features are consistent with their statistical significance listed in Table 5, with only the A2–N2 forcing reaching the 95% confidence level. The responses of near-surface temperature (Fig. 7b) to ozone forcing and, in particular, to sulfate direct forcing are again not significant; whereas the responses to indirect forcing of A2–N2 are distinctly larger than the internal variability (within 0.04 K) except one data point, for which year the near-surface temperature still decreases but the amplitude is too small to be regarded as significant. This outlier lowered the certainty of temperature responses, but the statistical significance still reached 95% (Table 5). The responses in cloud fraction and precipitation change are all indistinguishable from the internal variability, thus their statistical significance are low. Note that the internal variability in shortwave radiation and surface temperature from simulations of the A-series are a bit smaller than from N-series, so the above discussion is based on a stricter standard.

Sulfate itself also responds to the forcing it created, such as changes in circulation and transport patterns, as well as in-cloud chemical production and rain scavenging. As mentioned before, for such feedbacks we need to compare the results of A2–A0 (or A2–A1) instead of A2–N2 or A1–N1. Figure 7c shows that A2–A0, A2–A1, N2–N0 and N2–N1 give responses in sulfate loading consistently on the negative side (the behavior of A2–A1 is quite similar to that of A2–A0 thus are not shown). However, the annual variability of sulfate loading in N0 may sometimes exceed the responses in N2–N0 (from about  $-0.1$  to  $-0.4 \text{ mg S m}^{-2}$ ). Therefore, even though their statistical significance all reached 95% confidence, only the responses in A2–A0, A2–A1 and N2–N1 can be regarded as having clear-cut signals. Note that the annual variations of sulfate loading (in  $\text{mg S m}^{-2}$ ) are the largest for N0 ( $-0.1$  to  $+1.7$ ) and decrease

[Title Page](#)[Abstract](#)[Introduction](#)[Conclusions](#)[References](#)[Tables](#)[Figures](#)[⏪](#)[⏩](#)[◀](#)[▶](#)[Back](#)[Close](#)[Full Screen / Esc](#)[Printer-friendly Version](#)[Interactive Discussion](#)

progressively to  $\pm 0.04$  for A0,  $\pm 0.03$  for A1, and  $\pm 0.02$  for both A2 and N2. So, if we take the minuend (e.g., N2 in N2–N0) as the reference instead, the responses from N2–N0 would also be regarded as distinctly evident. The magnitude of annual variations seems to decrease with the degree of complexity in the simulation (e.g., with anthropogenic emissions, or with coupled direct or indirect effects). In other words, more controlling mechanisms may lead to a more stable sulfate loading. But the same does not apply to the internal variability of near-surface temperature, cloud fraction and precipitation, which remain similar among the simulations.

Another model uncertainty originates from the treatment of cloud drop effective radii. Recall that the A0 and N0 simulations applied prescribed cloud effective radii, with  $10\ \mu\text{m}$  over the ocean and  $5\ \mu\text{m}$  over the continent. Such a treatment gives radiative forcing very different from that calculated through the empirical formula (2). As can be seen from Table 4, the difference in all-sky radiation between N2 and N0 (A2 and A0) may reach  $8.2(9.8)\ \text{W m}^{-2}$ , which is much stronger than the indirect forcing of  $-1.69\ \text{W m}^{-2}$  that discussed earlier. Such differences do contain contributions from the direct aerosol forcing, but the effect should be small as can be seen from the clear-sky values. This implies that the model result is sensitive to the treatment of cloud drop effective radius and warrant the use of a more sophisticated scheme than using fixed values of 5 or  $10\ \mu\text{m}$ . Figure 8 shows the differences between results using the empirical formula and those with fixed effective radii. One can see that Eq. (2) gives stronger cloud forcing over the oceans but weaker forcing over most of the continents except the highly polluted area such as northeastern US and Europe in Fig. 8b. Therefore, the size range of effective radii across the continent and ocean is smaller than the specified range of 5 to  $10\ \mu\text{m}$  in N0 and A0, and this seems to be too narrow. We found that the inferred effective radii are still not much less than  $5\ \mu\text{m}$  even over polluted regions. Furthermore, the differences between A2 and A0 (Fig. 8b) are rather homogeneous over the continents thus of the geographic distribution of anthropogenic sulfate that shown in Fig. 3b is not reflected in the sulfate forcing. But over the oceans, the difference is prominent downwind of the pollution sources, indicating a more sensitive relationship

**Sulfur cycle and sulfate radiative forcing**

I.-C. Tsai et al.

Title Page

Abstract

Introduction

Conclusions

References

Tables

Figures

◀

▶

◀

▶

Back

Close

Full Screen / Esc

Printer-friendly Version

Interactive Discussion



between sulfur loading and effective radius.

The original coefficients for Eq. (2) from Boucher and Lohmann (1995) give much stronger dependences of cloud-drop number concentration on sulfate loading. When we apply them for the calculations in A2 and N2 (hereafter named A2B and N2B), the differences in cloud forcing indeed become obvious also over the polluted continents (Fig. 8d), while those for natural conditions in Fig. 8c remain similar in spatial distribution but lower in magnitude than those using the adjusted coefficients in Fig. 8a as they should be. However, the global sulfate forcing (A2B–N2B) now becomes  $-6.7 \text{ W m}^{-2}$ , which is much too high as compared with the estimations given in IPCC (2007). So, it is troublesome that the observation-based and seemingly more reasonable relationship between drop number and sulfate loading from Boucher and Lohmann (1995) overestimate the sulfate indirect forcing, whereas the relationship of Quass and Boucher (2005) that constrained total forcing (to give reasonable results) does not produce reasonable variations in effective radii. One possible explanation is that the incoming shortwave radiation sees mainly the cloud top, not deep inside the cloud or near the cloud base where the measurements of sulfate loading and cloud drop number were performed. Due to various number-reduction processes (such as coalescence, accretion or evaporation due to Bergeron-Findeisen conversion or entrainment mixing), the number of cloud drops tends to vary significantly with height. The microphysical properties near the top of clouds (particularly those high enough to be glaciated partly or fully) might not respond significantly to the change in sulfate loading. It is also possible that Eq. (2) is an oversimplification, as the cloud-drop number concentration actually depends on the size spectrum and chemical composition of the aerosol particles in addition to the strength of updraft. As both the constrained and un-constrained sulfate-effective-radius relationships may contain large uncertainties, more detailed treatment of aerosol-cloud interactions are needed in global climate models. Of course, deficiencies in other aspects of cloud representation in global-scale models cannot be ignored either.

**Sulfur cycle and sulfate radiative forcing**

I.-C. Tsai et al.

Title Page

Abstract

Introduction

Conclusions

References

Tables

Figures

◀

▶

◀

▶

Back

Close

Full Screen / Esc

Printer-friendly Version

Interactive Discussion



## 5 Conclusions

In this study, we incorporated a sulfur cycle scheme that interact on-line with an extensive gas phase scheme previously included, to take into account emissions, gas and liquid phase chemical processes, and deposition processes, into a Global Climate-Chemistry Model to study the sulfur cycle and the effect of sulfate aerosols on climate through scattering of solar radiation and change of cloud albedo. The coupling of aerosol and cloud radiation with the meteorology also allowed us to analyze response of the climate parameters and their feedback.

Under pre-industrial natural conditions, over 73% of the atmospheric  $\text{SO}_2$  is produced by DMS oxidation, the rest by volcanic activities. Whereas 87% of  $\text{SO}_2$  is converted to sulfate in the atmosphere, nearly all of the rest is removed by dry deposition. Sulfate is produced mainly by in-cloud oxidation (51% with ozone and 34% with  $\text{H}_2\text{O}_2$ ), and 92% of it is removed by wet deposition. Adding the 1985 anthropogenic emission, which accounts for 79% of the total  $\text{SO}_2$  production, global burden of  $\text{SO}_2$  and sulfate both nearly doubled. About 80% of  $\text{SO}_2$  convert to sulfate, and the weighting of sulfate production by in-cloud ozone oxidation increases to 56%, while the fractions by  $\text{H}_2\text{O}_2$  oxidation and gas-phase OH reaction decrease to 30% and 11%, respectively. Wet deposition is still the dominating sink for sulfate, accounting for 91% of the loss. Atmospheric lifetimes of  $\text{SO}_2$  and sulfate calculated from GCCM are 1.8 and 4.0 days, respectively, under natural conditions. The values become 1.0 and 2.4 days when anthropogenic emissions are included. The overall lifetime of sulfur ( $\text{SO}_2$  plus sulfate) is 5.3 days for natural conditions and 2.9 days with anthropogenic emission. Due to its rather short lifetime, anthropogenic  $\text{SO}_2$  stays mostly over the populated continents and the nearby oceans, as well as over the shipping corridors. Being a secondary compound and the more than doubled lifetime allows sulfate to disperse further downstream of the prevailing winds than  $\text{SO}_2$ . Anthropogenic sulfate can be transported to rather high altitudes. Over northern hemispheric mid-latitudes, more than 50% of the sulfate near the tropopause (at a height of 200 hPa) may be of anthropogenic origin.

### Sulfur cycle and sulfate radiative forcing

I.-C. Tsai et al.

Title Page

Abstract

Introduction

Conclusions

References

Tables

Figures

◀

▶

◀

▶

Back

Close

Full Screen / Esc

Printer-friendly Version

Interactive Discussion



Anthropogenic SO<sub>2</sub>, on the other hand, shows its dominance only below the 500 hPa level over the pollution sources.

With the 1985 emissions, global mean sulfate burden increased from the natural condition of 0.27 to 0.54 Tg S. The increase of sulfate may cause a reduction of global incoming solar radiation by about 0.47 W m<sup>-2</sup> from the direct scattering (under all-sky conditions), and by 1.69 W m<sup>-2</sup> from the enhancement of cloud albedo. Such radiative forcing may cause global mean temperature to decrease by a meager 0.02 and 0.09 K, respectively. Other climate parameters also seem to respond vaguely to sulfate forcing, such as the slight increase in global cloud fraction and reduction of global precipitation. Regional radiative forcing and temperature response can be much higher, reaching -7 W m<sup>-2</sup> and -0.6 K in Europe, -4 W m<sup>-2</sup> and -0.2 K in East Asia, and -5 W m<sup>-2</sup> and -0.2 K in North America, but the responses in clouds and precipitation can be quite different from the global mean, such as increasing cloudiness in Europe and North America but increasing clear sky in East Asia.

By designing a series of simulations that turn on and off the anthropogenic emissions or the aerosol effects, we demonstrated that climate signals from the direct forcing of sulfate are indistinguishable from the internal climate variability of the model. The indirect forcing, on the other hand, gives clear signals of climate responses. The indirect forcing of sulfate not only changed the meteorological fields but affected also sulfate itself. Global sulfate burden in the atmosphere would decrease by a few percent when the aerosol effects are coupled into the model. From a budget analysis, we found that this decrease is likely caused by an increase in precipitation thus wet deposition, as well as a reduction in vertical transport thus enhanced dry deposition of SO<sub>2</sub>, which then cause a reduction of aqueous-phase conversion into sulfate.

Note that we used the sulfur cycle and sulfate as the focus in studying the effects of chemistry-climate interaction. It is quite clear that the regional climate variability becomes an outstanding issue to address properly the interaction. In this regard, further study of using coupled atmosphere-ocean model is warranted. In addition, uncertainties in the treatment of aerosol-cloud interactions remain rather large, thus improve-

## Sulfur cycle and sulfate radiative forcing

I.-C. Tsai et al.

Title Page

Abstract

Introduction

Conclusions

References

Tables

Figures

◀

▶

◀

▶

Back

Close

Full Screen / Esc

Printer-friendly Version

Interactive Discussion



ments are deemed necessary for better understanding of the aerosol effect on global climate.

*Acknowledgements.* This research was supported by the research grants NSC 94-2752-M-002-012-PAE, NSC 95-2752-M-002-013-PAE, NSC 96-2752-M-002-013-PAE, NSC 97-2752-M-002-012-PAE, NSC 97-2111-M-002-002, and NSC 98-2111-M-002-001.

## References

Albrecht, B. A.: Aerosols, cloud microphysics, and fractional cloudiness, *Science*, 245, 1227–1230, 1989.

Amels, P., Elias, H., Götz, U., Steingens, U., and Wannowius, K. J.: Kinetic investigation of the stability of peroxyacetic acid and of its reaction with sulfur (IV) in aqueous solution, in: *Heterogeneous and Liquid Phase Processes*, Springer-Verlag, New York, 77–88, 1996.

Anderson, T. L., Charlson, R. J., Schwartz, S. E., Knutti, R., Boucher, O., Rodhe, H., and Heintzenberg, J.: Climate forcing by aerosols – a hazy picture, *Science*, 300, 1103–1104, 2003.

Audiffren, N., Buisson, E., Cautenet, S., and Chaumerliac, N.: Photolytic impact of a stratocumulus cloud layer upon the chemistry of an offshore advected plume of pollutants during the NARE 1993 intensive experiment: a numerical study, *Atmos. Res.*, 70, 89–108, 2004.

Benkovitz, C. M., Scholtz, M. T., Pacyna, J., Tarraso'n, L., Dignon, J., Voldner, E. C., Spiro, P. A., Logan, J. A., and Graedel, T. E.: Global gridded inventories of anthropogenic emissions of sulfur and nitrogen, *J. Geophys. Res.*, 101, 29239–29253, 1996.

Berglen T. F., Berntsen, T. K., Isaksen, I. S. A., and Sundet, J. K.: A global model of the coupled sulfur/oxidant chemistry in the troposphere: The sulfur cycle, *J. Geophys. Res.*, 109, D19310, doi:10.1029/2003JD003948, 2004.

Berntsen, T. K. and Isaksen, I. S. A.: A global 3-D chemical transport model for the troposphere; 1. Model description and CO and ozone results, *J. Geophys. Res.*, 102, 21239–21280, 1997.

Boucher, O. and Anderson, T. L.: General circulation model assessment of the sensitivity of direct climate forcing by anthropogenic sulfate aerosols to aerosol size and chemistry, *J. Geophys. Res.*, 100(D12), 26117–26134, 1995.

Boucher, O. and Lohmann, U.: The sulfate-CCN-cloud albedo effect: A sensitivity study with two general circulation models, *Tellus*, 47B, 281–300, 1995.

## Sulfur cycle and sulfate radiative forcing

I.-C. Tsai et al.

Title Page

Abstract

Introduction

Conclusions

References

Tables

Figures

◀

▶

◀

▶

Back

Close

Full Screen / Esc

Printer-friendly Version

Interactive Discussion





**Sulfur cycle and sulfate radiative forcing**

I.-C. Tsai et al.

Title Page

Abstract

Introduction

Conclusions

References

Tables

Figures

◀

▶

◀

▶

Back

Close

Full Screen / Esc

Printer-friendly Version

Interactive Discussion

- Cerveny, R. S. and Balling Jr., R. C.: Weekly cycles of air pollutants, precipitation and tropical cyclones in the coastal NW Atlantic region, *Nature*, 394, 561–563, 1998.
- Chen, Y. and Penner, J. E.: Uncertainty analysis for estimates of the first indirect aerosol effect, *Atmos. Chem. Phys.*, 5, 2935–2948, 2005,  
5 <http://www.atmos-chem-phys.net/5/2935/2005/>.
- Chin, M., Jacob, D. J., Gardner, G. M., Foreman-Fowler, M. S., Spiro, P. A., and Savoie, D. L.: A global three-dimensional model of tropospheric sulfate, *J. Geophys. Res.*, 101, 18667–18690, 1996.
- Chin, M., Savoie, D. L., Huebert, B. J., Bandy, A. R., Thornton, D. C., Bates, T. S., Quinn, P. K.,  
10 Saltzman, E. S., and De Bruyn, W. J.: Atmospheric sulfur cycle simulated in the global model GOCART: Comparison with field observations and regional budgets, *J. Geophys. Res.*, 105, 24689–24712, 2000.
- Chou, C., Neelin, J. D., Lohmann, U., and Feichter, J.: Local and remote impacts of aerosol climate forcing on tropical precipitation, *J. Climate*, 18, 4621–4636, 2005.
- 15 Chuang, C. C., Penner, J. E., Taylor, K. E., Grossman, A. S., and Walton, J. J.: An assessment of the radiative effects of anthropogenic sulfate, *J. Geophys. Res.*, 102(D3), 3761–3778, 1997.
- DeMore, W. B., Sander, S. P., Golden, D. M., Hampson, R. F., Kurylo, M. J., Howard, C. J., Ravishankara, A. R., Kolb, C. E., and Molina, M. J.: Chemical kinetics and photochemical data for use in stratospheric modeling, Tech. Rep. 97–4, Jet Propulsion Lab., Pasadena, Calif., 1997.
- 20 Endresen, Ø., Sørsgård, E., Sundet, J. K., Dalsøren, S. B., Isaksen, I. S. A., Berglen, T. F., and Gravir, G.: Emission from international sea transportation and environment impact, *J. Geophys. Res.*, 108(D17), 4560, doi:10.1029/2002JD002898, 2003.
- 25 Eyring, V., Köhler, H. W., van Aardenne, J., and Lauer, A.: Emission from international shipping: 1. The last 50 years, *J. Geophys. Res.*, 110, D17305, doi:10.1029/2004JD005619, 2005.
- Feichter, J., Kjellström, E., Rodhe, H., Dentener, F., Lelieveld, J., and Roelofs, G. J.: Simulation of the tropospheric sulfur cycle in a global climate model, *Atmos. Environ.*, 30(10–11), 1693–1707, 1996.
- 30 Gates, W. L., Boyle, J., Covey, C., Dease, C., Doutriaux, C., Drach, R., Fiorino, M., Gleckler, P., Hnilo, J., Marlais, S., Phillips, T., Potter, G., Santer, B., Sperber, K., Taylor, K., and Williams, D.: An overview of the results of the Atmospheric Model Intercomparison Project (AMIP I), *Bull. Am. Meteorol. Soc.*, 80, 29–55, 1999.





Ghan, S., Easter, R., Chapman, E., Abdul-Razzak, H., Zhang, Y., Leung, R., Laulainen, N., Saylor, R. D., and Zaveri, R.: A physically-based estimate of radiative forcing by anthropogenic sulphate aerosol, *J. Geophys. Res.*, 106(D6), 5279–5294, doi:10.1029/2000JD900503, 2001.

5 Graft, H., Feichter, J., and Langmann, B.: Volcanic sulfur emissions: Estimates of sources strength and its contribution to the global sulfate distribution, *J. Geophys. Res.*, 102, 10727–10738, 1997.

Gu, Y., Liou, K. N., Xue, Y., Mechoso, C. R., Li, W., and Luo, Y.: Climatic effects of different aerosol types in China simulated by the UCLA general circulation model, *J. Geophys. Res.*, 111, D15201, doi:10.1029/2005JD006312, 2006.

10 Hack, J. J., Kiehl, J. T., and Hurrell, J. W.: The hydrologic and thermodynamic characteristics of the NCAR CCM3, *J. Climate*, 11, 1179–1206, 1998.

Hansen, J., Sato, M., and Ruedy, R.: Radiative forcing and climate response, *J. Geophys. Res.*, 102(D6), 6831–6864, 1997.

15 Haywood, J. M. and Shine, K. P.: Multi-spectral calculations of the direct radiative forcing of tropospheric sulphate and soot aerosols using a column model, *Q. J. Roy. Meteorol. Soc.*, 123, 1907–1930, 1997.

Haywood, J. M., Ramaswamy, V., and Soden, B. J.: Tropospheric aerosol climate forcing in clear-sky satellite observations over the oceans, *Science*, 283, 1299–1305, 1999.

20 Huang, Y., Chameides, W. L., and Dickinson, R. E.: Direct and indirect effects of anthropogenic aerosols on regional precipitation over east Asia, *J. Geophys. Res.*, 112, D03212, doi:10.1029/2006JD007114, 2007.

IPCC: Climate Change 2007: The Physical Science Basis. Contribution of Working Group I to the Fourth Assessment Report of the Intergovernmental Panel on Climate Change, edited by: Solomon, S., Qin, D., Manning, M., Chen, Z., Marquis, M., Averyt, K. B., Tignor, M., and Miller, H. L., Cambridge Univ. Press, Cambridge, UK, and New York, USA, 2007.

Isaksen, I. S. A. and Hov, Ø.: Calculations of trends in the tropospheric concentrations of O<sub>3</sub>, OH, CO, CH<sub>4</sub>, and NO<sub>x</sub>, *Tellus B*, 39, 271–283, 1987.

25 Iversen, T., Kirkevåg, A., Kristjansson, J. E., and Seland, Ø.: Climate effects of sulphate and black carbon estimated in a global climate model. in: *Air Pollution Modeling and its Application XIV*, Kluwer/Plenum Publishers, New York, 335–342, 2000.

30 Iversen, T. and Seland, Ø.: A scheme for process-tagged SO<sub>4</sub> and BC aerosols in NCAR CCM3: Validation and sensitivity to cloud processes, *J. Geophys. Res.*, 107(D24), 4751,

---

## Sulfur cycle and sulfate radiative forcing

I.-C. Tsai et al.

---

Title Page

Abstract

Introduction

Conclusions

References

Tables

Figures

◀

▶

◀

▶

Back

Close

Full Screen / Esc

Printer-friendly Version

Interactive Discussion



doi:10.1029/2001JD000885, 2002.

Jacobson, M. Z.: Global direct radiative forcing due to multicomponent anthropogenic and natural aerosols, *J. Geophys. Res.*, 106, 1551–1568, 2001.

Jones, A., Roberts, D. L., and Woodage, M. J.: Indirect sulphate aerosol forcing in a climate model with an interactive sulfur cycle, *J. Geophys. Res.*, 106, 20293–20310, 2001.

Jones, A., Haywood, J. M., and Boucher, O.: Aerosol forcing, climate response and climate sensitivity in the Hadley Centre climate model, *J. Geophys. Res.*, 112, D20211, doi:10.1029/2007JD008688, 2007.

Kaufman, Y. J. and Fraser, R. S.: The effect of smoke particles on clouds and climate forcing, *Science*, 277(5332), 1636–1638, 1997.

Kettle, A. J., Andreae, M. O., Amouroux, D., Andreae, T. W., Bates, T. S., Berresheim, H., Bingemer, H., Boniforti, R., Curran, M. A. J., DiTullio, G. R., Helas, G., Jones, G. B., Keller, M. D., Kiene, R. P., Leck, C., Lévassieur, M., Malin, G., Maspero, M., Matrai, P., McTaggart, A. R., Mihalopoulos, N., Nguyen, B. C., Novo, A., Putaud, J. P., Rapsomanikis, S., Roberts, G., Schebeske, G., Sharma, S., Simó, R., Staubes, R., Turner, S., and Uher, G.: A global database of sea surface dimethylsulfide (DMS) measurements and a procedure to predict sea surface DMS as a function of latitude, longitude and month, *Global Biogeochem. Cy.*, 13(2), 399–444, 1999.

Kettle, A. J. and Andreae, M. O.: Flux of dimethylsulfide from the oceans: A comparison of updated data seas and flux models, *J. Geophys. Res.*, 105(D22), 26793–26808, 399–444, 2000.

Kiehl, J. T. and Briegleb, B. P.: The relative roles of sulfate aerosols and greenhouse gases in climate forcing, *Science*, 260, 311–314, 1993.

Kiehl, J. T. and Rodhe, H.: Modeling geographical and seasonal forcing due to aerosols, in: *Aerosol Forcing of Climate*, J. Wiley and Sons Ltd, 281–296, 1995.

Kiehl, J. T., Schneider, T. L., Rasch, P. J., Barth, M. C., and Wong, J.: Radiative forcing due to sulfate aerosols from simulations with the National Center for Atmospheric Research Community Climate Model, Version 3, *J. Geophys. Res.*, 105(D1), 1441–1457, 2000.

Koch, D., Jacob, D. J., Tegen, I., Rind, D., and Chin, M.: Tropospheric sulfur simulation and sulfate direct radiative forcing in the Goddard Institute for Space Studies general circulation model, *J. Geophys. Res.*, 104, 23799–23822, 1999.

Koch, D.: Transport and direct radiative forcing of carbonaceous and sulfate aerosols in the GISS GCM, *J. Geophys. Res.*, 106(D17), 20311–20332, 2001.

**Sulfur cycle and sulfate radiative forcing**

I.-C. Tsai et al.

Title Page

Abstract

Introduction

Conclusions

References

Tables

Figures

◀

▶

◀

▶

Back

Close

Full Screen / Esc

Printer-friendly Version

Interactive Discussion



**Sulfur cycle and sulfate radiative forcing**

I.-C. Tsai et al.

Title Page

Abstract

Introduction

Conclusions

References

Tables

Figures

◀

▶

◀

▶

Back

Close

Full Screen / Esc

Printer-friendly Version

Interactive Discussion



- Langner, J. and Rodhe, H.: A global three-dimensional model of the tropospheric sulfur cycle, *J. Atmos. Chem.*, 13, 225–263, 1991.
- Lau, K.-M., Kim, J. H., and Sud, Y.: Intercomparison of hydrological processes in AMIP GCMs, *Bull. Am. Meteorol. Soc.*, 77, 2209–2227, 1996.
- 5 Lelieveld, J.: Modeling of heterogeneous chemistry in the global troposphere. In: *Chemistry of Aquatic Systems: Local and Global perspective*, Kluwer Academic Publ., Dordrecht, 73–95, 1994.
- Liss, P. S. and Merlivat, L.: Air-sea gas exchange rates: Introduction and synthesis, in: *The Role of Air-Sea Exchange in Geochemical Cycling*, D. Reidel, Norwell, Mass., 113–127, 10 1986.
- Liu, Y., Sun, J., and Yang, B.: The Effects of black carbon and sulfate aerosols in China regions on East Asia monsoons, *Tellus B*, 61(4), 642–656, 2009.
- Lohmann, U. and Feichter, J.: Global indirect aerosol effects: a review, *Atmos. Chem. Phys.*, 5, 715–737, 2005, 15 <http://www.atmos-chem-phys.net/5/715/2005/>.
- Martin, G. M., Johnson, D. W., and Spice, A.: The measurements and parameterization of effective radius of droplets in warm stratocumulus clouds, *J. Atmos. Sci.*, 51, 1823–1842, 1994.
- Martin, L. R. and Damschen, D. E.: Aqueous oxidation of sulfur dioxide by hydrogen peroxide at low pH, *Atmos. Environ.*, 15, 1615–1621, 1981. 20
- Mickley, L. J., Murti, P. P., Jacob, D. J., Logan, J. A., Koch, D. M., and Rind, D.: Radiative forcing from tropospheric ozone calculated with a unified chemistry-climate model, *J. Geophys. Res.*, 104, 30153–30172, 1999.
- Mitchell, J. F. B., Johns, T. C., Gregory, J. M., and Tett, F. B.: Climate response to increasing levels of greenhouse gases and sulphate aerosols, *Nature*, 376, 501–504, 1995. 25
- Moller, D.: Kinetic model of atmospheric SO<sub>2</sub> oxidation based on published data, *Atmos. Environ.*, 14, 1067–1076, 1980.
- Myhre, G., Stordal, F., Restad, K., and Isaksen, I. S. A.: Estimation of the direct radiative forcing due to sulphate and soot aerosols, *Tellus*, 50B, 463–477, 1998.
- 30 Jöckel, P., Sander, R., Kerkweg, A., Tost, H., and Lelieveld, J.: Technical Note: The Modular Earth Submodel System (MESSy) – a new approach towards Earth System Modeling, *Atmos. Chem. Phys.*, 5, 433–444, 2005, <http://www.atmos-chem-phys.net/5/433/2005/>.

- Penner, J. E., Chuang, C. C., and Grant, K.: Climate forcing by carbonaceous and sulphate aerosols, *Clim. Dynam.*, 14, 839–851, 1998
- Quaas, J. and Boucher, O.: Constraining the first aerosol indirect radiative forcing in the LMDZ GCM using POLDER and MODIS satellite data, *Geophys. Res. Lett.*, 32, L17814, doi:10.1029/2005GL023850, 2005.
- Ramanathan, V., Crutzen, P. J., Kiehl, J. T., and Rosenfeld, D.: Aerosols, climate, and the hydrological cycle, *Science*, 294, 2119–2124, 2001.
- Restad, K., Isaksen, I. S. A., and Berntsen, T. K.: Global distribution of sulfate in the troposphere: A three-dimensional model study, *Atmos. Environ.*, 32, 3593–3609, 1998.
- Rodhe, H., and Isaksen, I. S. A.: Global distribution of sulfur compounds in the troposphere estimated in a height/latitude transport model, *J. Geophys. Res.*, 85, 7401–7409, 1980.
- Roelofs, G.-J., Lelieveld, J., and Ganzeveld, L.: Simulation of global sulfate distribution and the influence on effective cloud drop radii with a coupled photochemistry-sulfur cycle model, *Tellus B*, 50, 224–242, 1998.
- Rosenfeld, D.: Suppression of rain and snow by urban and industrial air pollution, *Science*, 287(5459), 1793–1796, 2000.
- Rotstajn, L. D. and Penner, J. E.: Indirect aerosol forcing, quasi-forcing, and climate response, *J. Climate*, 14, 2960–2975, 2001.
- Schulz, M., Textor, C., Kinne, S., Balkanski, Y., Bauer, S., Berntsen, T., Berglen, T., Boucher, O., Dentener, F., Guibert, S., Isaksen, I. S. A., Iversen, T., Koch, D., Kirkevåg, A., Liu, X., Montanaro, V., Myhre, G., Penner, J. E., Pitari, G., Reddy, S., Seland, Ø., Stier, P., and Takemura, T.: Radiative forcing by aerosols as derived from the AeroCom present-day and pre-industrial simulations, *Atmos. Chem. Phys.*, 6, 5225–5246, 2006, <http://www.atmos-chem-phys.net/6/5225/2006/>.
- Senior, C. A. and Mitchell, J. F. B.: Carbon dioxide and climate: The impact of cloud parameterization, *J. Climate*, 6, 393–418, 1993.
- Shindell, D. T., Grenfell, J. L., Rind, D., Grewe, V., and Price, C.: Chemistry-climate interaction in the GISS general circulation model: 1. Tropospheric chemistry model description and evaluation, *J. Geophys. Res.*, 106, 8047–8076, 2001.
- Spiro, P. A., Jacob, D. J., and Logan, J. A.: Global inventory of sulfur emission with 1°×1° resolution, *J. Geophys. Res.*, 97, 6023–6036, 1992.
- Twomey, S.: Pollution and the planetary albedo, *Atmos. Environ.*, 8, 1251–1256, 1974.
- Van Dorland, R., Dentener, F. J., and Lelieveld, J.: Radiative forcing due to tropospheric ozone

**Sulfur cycle and sulfate radiative forcing**

I.-C. Tsai et al.

Title Page

Abstract

Introduction

Conclusions

References

Tables

Figures

◀

▶

◀

▶

Back

Close

Full Screen / Esc

Printer-friendly Version

Interactive Discussion



- and sulfate aerosols, *J. Geophys. Res.*, 102(D23), 28079–28100, 1997.
- Williams, K. D., Jones, A., Roberts, D. L., Senior, C. A., and Woodage, M. J.: The response of the climate system to the indirect effects of anthropogenic sulfate aerosols, *Clim. Dynam.*, 17, 845–856, 2001.
- 5 Wang, W.-C., Liang, X. Z., Dudek, M. P., Pollard, D., and Thompson, S. L.: Atmospheric ozone as a climate gas, *Atmos. Res.*, 37, 247–256, 1995.
- Wong, S. and Wang, W.-C.: Interhemispheric asymmetry in the seasonal variation of the zonal mean tropopause, *J. Geophys. Res.*, 105, 26645–26659, 2000.
- Wong, S. and Wang, W.-C.: Tropical-extratropical connection in interannual variation of the tropopause: Comparison between NCEP/NCAR reanalysis and an atmospheric general cir-  
10 culation model, *J. Geophys. Res.*, 108(D2), 4043, doi:10.1029/2001JD002016, 2003.
- Wong, S., Wang, W.-C., Isaksen, I. S. A., Berntsen T. K., and Sundet, J. K.: A global climate-chemistry model study of present-day tropospheric chemistry and radiative forcing from changes in tropospheric O<sub>3</sub> since the preindustrial period, *J. Geophys. Res.*, 109, D11309,  
15 doi:10.1029/2003JD003998, 2004.
- Zhang, Y.: Online-coupled meteorology and chemistry models: history, current status, and outlook, *Atmos. Chem. Phys.*, 8, 2895–2932, 2008, <http://www.atmos-chem-phys.net/8/2895/2008/>.

---

**Sulfur cycle and  
sulfate radiative  
forcing**I.-C. Tsai et al.

---

[Title Page](#)[Abstract](#)[Introduction](#)[Conclusions](#)[References](#)[Tables](#)[Figures](#)[I◀](#)[▶I](#)[◀](#)[▶](#)[Back](#)[Close](#)[Full Screen / Esc](#)[Printer-friendly Version](#)[Interactive Discussion](#)

**Table 1.** Gaseous- and aqueous-phase reactions considered in the sulfur cycle.

Reaction	Reaction rate
Gas phase reaction <sup>a</sup>	
DMS + NO <sub>3</sub> → SO <sub>2</sub>	$k = 1.9 \times 10^{-13} \times \exp\left(\frac{520}{T}\right)$
OH + DMS → H <sub>2</sub> O + CH <sub>3</sub> SCH <sub>2</sub> → SO <sub>2</sub>	$k = 1.2 \times 10^{-11} \times \exp\left(\frac{-260}{T}\right)$
OH + DMS → CH <sub>3</sub> S(OH)CH <sub>3</sub> → 0.75SO <sub>2</sub> + 0.25MSA	$k = \left\{ [\text{O}_2] \times 1.7 \times 10^{-42} \times \exp\left(\frac{7810}{T}\right) \right\} / \left\{ 1 + [\text{O}_2] \times 5.5 \times 10^{-31} \times \exp\left(\frac{7460}{T}\right) \right\}$
SO <sub>2</sub> + OH → H <sub>2</sub> SO <sub>4</sub>	$k_{\text{OH}} = \left( \frac{k_0}{1 + \frac{k_0}{k_\infty}} \right) \times 0.6^{\{1 + [\log(k_0/k_\infty)]^2\}} - 1$ $k_0 = 3.0 \times 10^{-31} \times \left(\frac{300}{T}\right)^{3.3} \times [\text{M}]$ $k_\infty = 1.5 \times 10^{-12}$
Aqueous phase reaction	
H <sub>2</sub> O <sub>2</sub> (aq) + HSO <sub>3</sub> <sup>-</sup> (aq) ↔ H <sup>+</sup> (aq) + SO <sub>4</sub> <sup>2-</sup> (aq) + H <sub>2</sub> O	$k_{\text{H}_2\text{O}_2} = \frac{8.0 \times 10^4 \times \exp(-3650 \times T_f)}{0.1 + [\text{H}^+]}$ <sup>b</sup>
O <sub>3</sub> (aq) + SO <sub>3</sub> <sup>2-</sup> (aq) ↔ SO <sub>4</sub> <sup>2-</sup> (aq) + O <sub>2</sub> (aq)	$k_{\text{O}_3} = 1.8 \times 10^4 \times [\text{H}^+]^{-0.4}$ <sup>c</sup>
HO <sub>2</sub> NO <sub>2</sub> (aq) + HSO <sub>3</sub> <sup>-</sup> (aq) ↔ 2H <sup>+</sup> (aq) + SO <sub>4</sub> <sup>2-</sup> (aq) + NO <sub>3</sub> <sup>-</sup>	$k_{\text{HO}_2\text{NO}_2} = 3.1 \times 10^5$ <sup>d</sup>

$T$ : Temperature,  $T_f = 1/T - 1/298$ ,  $[\text{M}]$ : concentration of air,  $[\text{H}^+]$ : concentration of H<sup>+</sup>, assumed as  $3.16 \times 10^{-5}$ , i.e., pH=4.5.

<sup>a</sup> rates are from De More et al. (1997)

<sup>b</sup> unit is mol/L/s, from Martin and Damschen (1976)

<sup>c</sup> unit is mol/L/s, from Moller (1980)

<sup>d</sup> unit is mol/L/s, from Amels et al. (1996)

## Sulfur cycle and sulfate radiative forcing

I.-C. Tsai et al.

Title Page

Abstract

Introduction

Conclusions

References

Tables

Figures

◀

▶

◀

▶

Back

Close

Full Screen / Esc

Printer-friendly Version

Interactive Discussion



**Sulfur cycle and sulfate radiative forcing**

I.-C. Tsai et al.

**Table 2.** SO<sub>2</sub> global emission used in GCCM.

Type		Strength, Tg S yr <sup>-1</sup>
1985GEIA emission	>100 m	2.94
	<100 m	24.03
Biomass burning emission		2.24
Ship emission		3.41
Volcanic emission		8

[Title Page](#)[Abstract](#)[Introduction](#)[Conclusions](#)[References](#)[Tables](#)[Figures](#)[I◀](#)[▶I](#)[◀](#)[▶](#)[Back](#)[Close](#)[Full Screen / Esc](#)[Printer-friendly Version](#)[Interactive Discussion](#)

## Sulfur cycle and sulfate radiative forcing

I.-C. Tsai et al.

**Table 3.** Global sulfur burden (in Tg S) calculated from different sets of GCM simulations and comparison with those from a few models that also applied the 1985 GEIA emission inventory.

	N0	N1	N2	A0	A1	A2	a	b	c	d	e
SO <sub>2</sub>	0.15	0.15	0.15	0.30	0.29	0.29	0.26	0.34	0.42	0.56	0.61
Sulfate	0.30	0.28	0.27	0.55	0.55	0.54	0.50	0.53	0.62	0.73	0.96

a: Berglen et al. (2004); b: Chin et al. (1996); c: Restad et al. (1998); d: Koch et al. (1999); e: Roelofs et al. (1998).

[Title Page](#)
[Abstract](#)
[Introduction](#)
[Conclusions](#)
[References](#)
[Tables](#)
[Figures](#)
[Back](#)
[Close](#)
[Full Screen / Esc](#)
[Printer-friendly Version](#)
[Interactive Discussion](#)




**Sulfur cycle and sulfate radiative forcing**

I.-C. Tsai et al.

**Table 4.** Differences of global-mean radiative forcing (in  $\text{W m}^{-2}$ ) between simulations at the surface and top of atmosphere (TOA) under both clear-sky and all-sky conditions.

	Clear sky	All sky
A0–N0	–0.05	–0.14
A1–N1	–0.32	–0.14
A2–N2	–0.47	–1.69
N1–N0	–0.42	–0.36
A1–A0	–0.68	–0.35
N2–N0	–0.07	–8.21
A2–A0	–0.47	–9.77

[Title Page](#)[Abstract](#)[Introduction](#)[Conclusions](#)[References](#)[Tables](#)[Figures](#)[I◀](#)[▶I](#)[◀](#)[▶](#)[Back](#)[Close](#)[Full Screen / Esc](#)[Printer-friendly Version](#)[Interactive Discussion](#)

**Table 5.** Simulated shortwave radiative forcing and meteorological responses over the globe. Statistical significance under a two tailed test on the monthly values is given in the parentheses (only those greater than 75% are listed). Also listed at the bottom are simulated total cloud coverage and precipitation as a reference for comparison.

Radiative forcing ( $\text{W m}^{-2}$ )	A0–N0	−0.15	(70%)
	A1–N1	−0.14	(70%)
	A2–N2	−1.69	(95%)
Temperature change (K)	A0–N0	−0.04	(90%)
	A1–N1	−0.02	
	A2–N2	−0.09	(95%)
Cloud fraction change	A0–N0	0.0001	
	A1–N1	0.0007	
	A2–N2	0.0004	
Precipitation change ratio	A0–N0	0.02%	
	A1–N1	−0.08%	
	A2–N2	−0.21%	(70%)
Cloud fraction	A0	0.603	
	A1	0.603	
	A2	0.601	
Precipitation (mm/day)	A0	3.16	
	A1	3.15	
	A2	3.18	

## Sulfur cycle and sulfate radiative forcing

I.-C. Tsai et al.

Title Page

Abstract

Introduction

Conclusions

References

Tables

Figures

◀

▶

◀

▶

Back

Close

Full Screen / Esc

Printer-friendly Version

Interactive Discussion



## Sulfur cycle and sulfate radiative forcing

I.-C. Tsai et al.

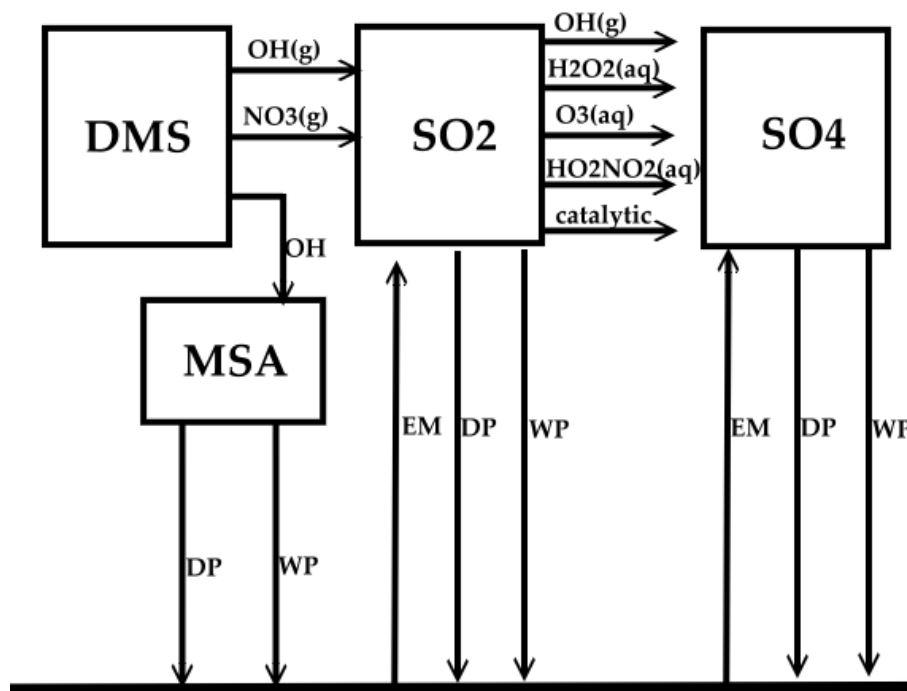


**Fig. 1.** Sulfur cycle in GCM. Four species including DMS, MSA, SO<sub>2</sub> and sulfate are included. The arrows are different fluxes including emission (EM), dry deposition (DP) and wet deposition (WP) and gas phase (g) and aqueous phase (aq) reactions.

[Title Page](#)[Abstract](#)[Introduction](#)[Conclusions](#)[References](#)[Tables](#)[Figures](#)[◀](#)[▶](#)[◀](#)[▶](#)[Back](#)[Close](#)[Full Screen / Esc](#)[Printer-friendly Version](#)[Interactive Discussion](#)

## Sulfur cycle and sulfate radiative forcing

I.-C. Tsai et al.

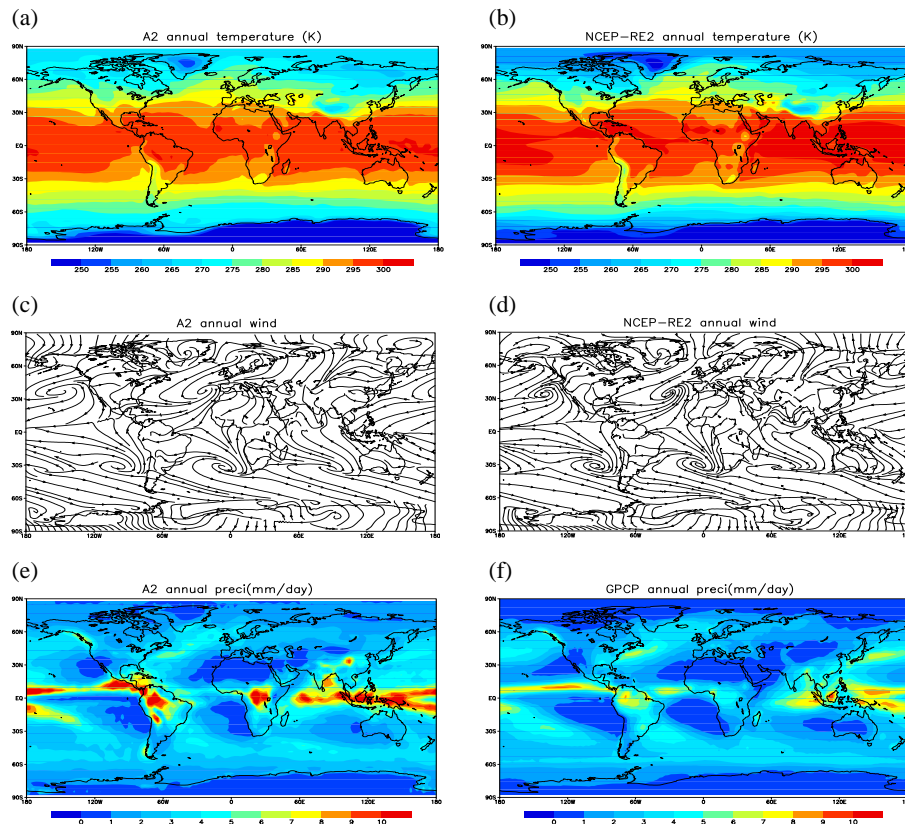


**Fig. 2.** Comparison of meteorological fields from the A2 simulation (left panels) with those from observation or reanalysis data (right panels). Top: near surface temperature (K); Middle: near-surface streamline; Bottom: precipitation (in  $\text{mm day}^{-1}$ ).

[Title Page](#)[Abstract](#)[Introduction](#)[Conclusions](#)[References](#)[Tables](#)[Figures](#)[◀](#)[▶](#)[◀](#)[▶](#)[Back](#)[Close](#)[Full Screen / Esc](#)[Printer-friendly Version](#)[Interactive Discussion](#)

## Sulfur cycle and sulfate radiative forcing

I.-C. Tsai et al.

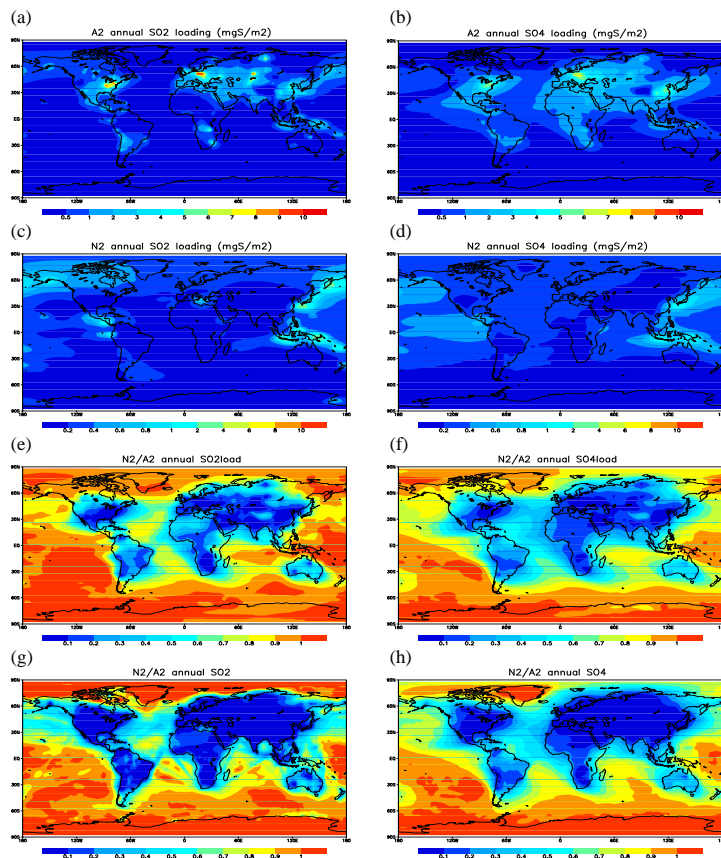


**Fig. 3.** Comparison of the global distribution of SO<sub>2</sub> (left) and sulfate (right) from GCM simulations. Top row: column loading (in mg S m<sup>-2</sup>) from the A2 simulation; Second row: column loading (in mg S m<sup>-2</sup>) from the N2 simulation; Third row: ratio of natural to total (N2:A2) column loading; Bottom row: ratio of natural to total (N2:A2) concentration near the surface.

[Title Page](#)[Abstract](#)[Introduction](#)[Conclusions](#)[References](#)[Tables](#)[Figures](#)[◀](#)[▶](#)[◀](#)[▶](#)[Back](#)[Close](#)[Full Screen / Esc](#)[Printer-friendly Version](#)[Interactive Discussion](#)

Sulfur cycle and  
sulfate radiative forcing

I.-C. Tsai et al.

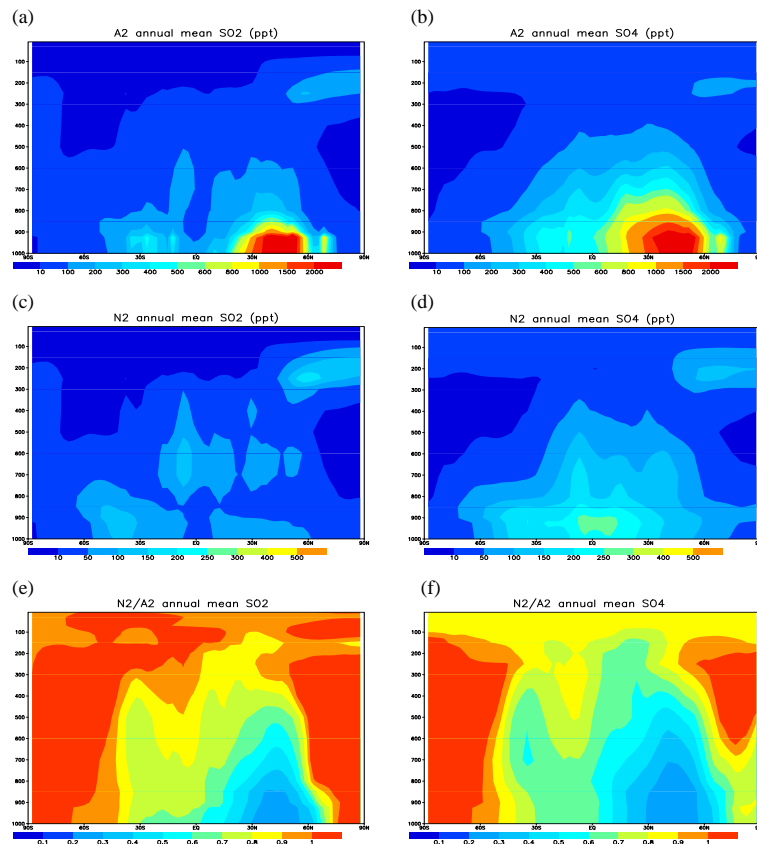


**Fig. 4.** Comparison of the vertical profiles of zonal-mean SO<sub>2</sub> (left) and sulfate (right) concentrations. Top: concentration (in ppt) under polluted conditions (A2); Middle: concentration (in ppt) under natural conditions (N2); Bottom: ratio of natural to total (N2:A2) concentrations.

[Title Page](#)[Abstract](#)[Introduction](#)[Conclusions](#)[References](#)[Tables](#)[Figures](#)[◀](#)[▶](#)[◀](#)[▶](#)[Back](#)[Close](#)[Full Screen / Esc](#)[Printer-friendly Version](#)[Interactive Discussion](#)

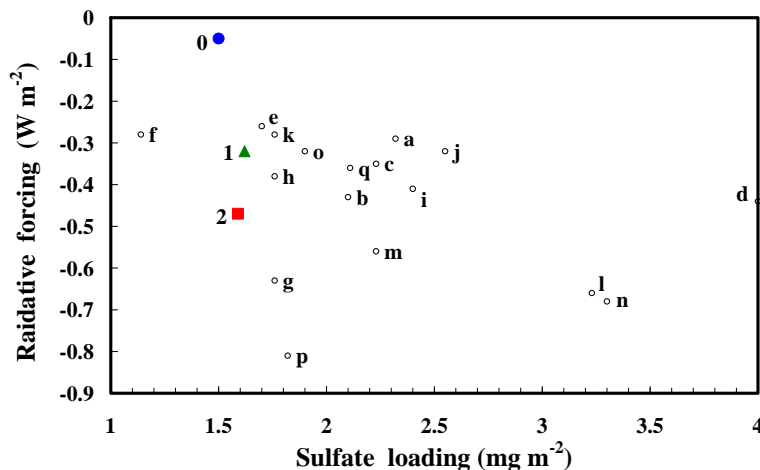


**Fig. 5.** Comparison of sulfate burden and direct effect between GCCM and other model results. The filled circle, triangle and square represent the GCCM results of A0–N0 (blue circle labeled “0”), A1–N1 (green triangle labeled “1”) and A2–N2 (red square labeled “2”), respectively. The letters next to the open circles indicate results from the following studies: (a). Boucher and Anderson (1995), (b), Chuang et al. (1997), (c) Feichter et al. (1997), (d) Ghan et al. (2001a), (e) Graf et al. (1997), (f) Hansen et al. (1998), (g) Haywood and Ramaswamy (1998), (h) Haywood et al. (1997a), (i) Iversen et al. (2000), (j) Jacobson (2001), (k) Kiehl and Briegleb (1993), (l) Kiehl and Rodhe (1995), (m) Kiehl et al. (2000), (n) Koch et al. (1999), (o) Myhre et al. (1998c), (p) Penner et al. (1998b), (q) van Dorland et al. (1997).

## Sulfur cycle and sulfate radiative forcing

I.-C. Tsai et al.

Title Page

Abstract

Introduction

Conclusions

References

Tables

Figures

◀

▶

◀

▶

Back

Close

Full Screen / Esc

Printer-friendly Version

Interactive Discussion



**Sulfur cycle and sulfate radiative forcing**

I.-C. Tsai et al.

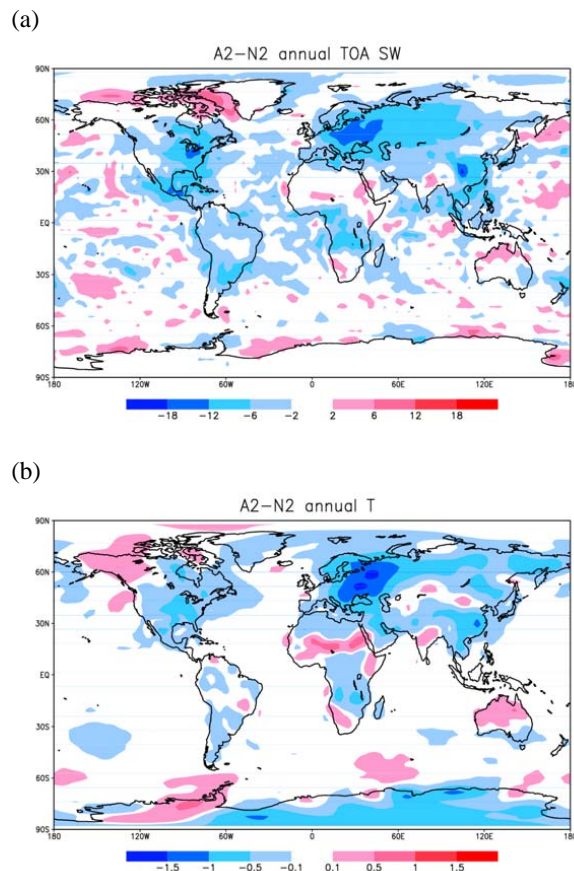


**Fig. 6.** Anthropogenic sulfate forcing and climate response from the A2–N2 results. Top: radiative forcing at TOA (in  $\text{W m}^{-2}$ ). Bottom: near-surface air temperature change (in K). Negative values are indicated in gray shading, while positive values are marked with contours.

[Title Page](#)[Abstract](#)[Introduction](#)[Conclusions](#)[References](#)[Tables](#)[Figures](#)[◀](#)[▶](#)[◀](#)[▶](#)[Back](#)[Close](#)[Full Screen / Esc](#)[Printer-friendly Version](#)[Interactive Discussion](#)



## Sulfur cycle and sulfate radiative forcing

I.-C. Tsai et al.

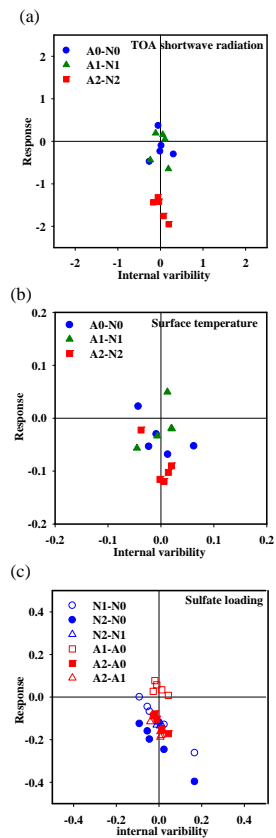


**Fig. 7.** Comparison between model internal variability (abscissa) and responses to sulfate forcing (ordinate). **(a)** Global mean TOA radiative forcing (in  $\text{W m}^{-2}$ ); **(b)** near-surface temperature (in K); and **(c)** sulfate loading (in  $\text{mg S m}^{-2}$ ). The internal variability is defined as the annual variation of the reference case, which is chosen as the subtrahend of the two simulations being compared (e.g., N0 in N2–N0).

[Title Page](#)[Abstract](#)[Introduction](#)[Conclusions](#)[References](#)[Tables](#)[Figures](#)[◀](#)[▶](#)[◀](#)[▶](#)[Back](#)[Close](#)[Full Screen / Esc](#)[Printer-friendly Version](#)[Interactive Discussion](#)

## Sulfur cycle and sulfate radiative forcing

I.-C. Tsai et al.

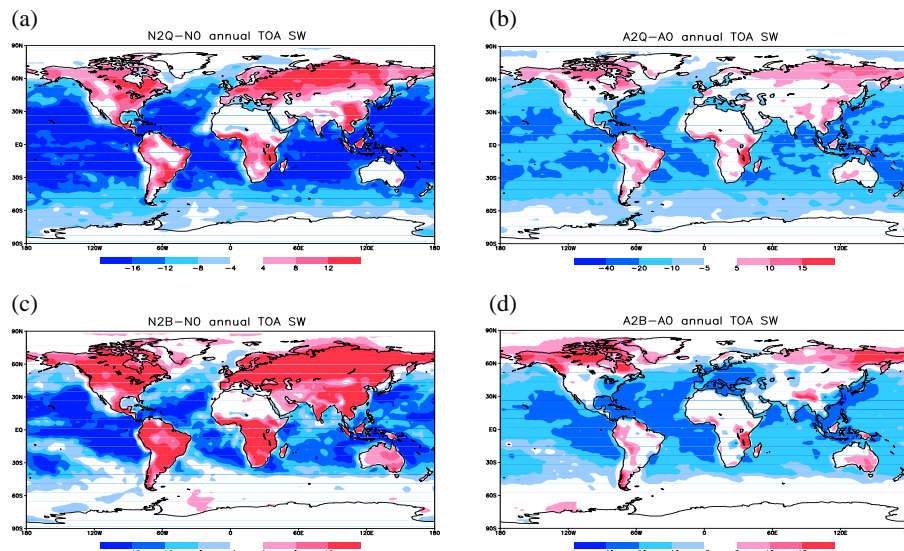


**Fig. 8.** Differences in all-sky shortwave radiation between simulations using the empirical formula (2) and those with specified effective radii. **(a)** N2–N0, **(b)** A2–A0, **(c)** N2B–N0, and **(d)** A2B–A0. A2 and N2 applied the coefficients from Quass and Boucher (2005), whereas A2B and B2B applied those from Boucher and Lohmann (1995). The white line marks the zero isopleths.

[Title Page](#)[Abstract](#)[Introduction](#)[Conclusions](#)[References](#)[Tables](#)[Figures](#)[◀](#)[▶](#)[◀](#)[▶](#)[Back](#)[Close](#)[Full Screen / Esc](#)[Printer-friendly Version](#)[Interactive Discussion](#)